# Tomographic Electrical Resistance-based Damage Sensing in Nano-Engineered Composite Structures

Sunny S. Wicks[1], Roberto Guzman deVilloria[2] and Brian L. Wardle[3]
*Massachusetts Institute of Technology, Cambridge, MA 02139*

Ajay Raghavan[4] and Seth Kessler[5]
*Metis Design Corporation, Cambridge, MA 02141*

**Aligned carbon nanotubes (CNTs) are being investigated as a means for enhancing structural performance of composite structures. Inherent in introducing CNTs into existing polymer-matrix composites are new multifunctional attributes such as significantly enhanced electrical conductivity and piezoresistivity that may be used for damage sensing and inspection. Here, fiber-reinforced polymer-matrix laminates with *aligned* CNTs grown *in-situ* are coupled with a non-invasive sensing scheme utilizing the enhanced electrical conductivity of the laminates to infer damage based on resistance changes. The laminates contain long (~10 micron) aligned CNTs throughout the woven plies of the laminate, including at the ply interfaces. Electrodes are written onto the laminate surfaces using a direct-write process, and 3D damage inspection (in-plane and through-thickness) is demonstrated for impacted composite plates.**

## Nomenclature

*CNT* = carbon nanotube
*CVD* = chemical vapor deposition
*FFRP* = fuzzy fiber reinforced plastic
*NDE/I* = non-destructive evaluation/inspection
*SHM* = structural health monitoring

## I. Introduction

Advanced composite materials are increasingly replacing metals in the aerospace industry as they offer weight-saving improvements, such as high specific strength and stiffness, while providing resistance to fatigue and corrosion. Traditional advanced composites, however, exhibit significantly reduced electrical and thermal conductivity relative to metals, and matrix-rich regions at ply interfaces results in relatively poor interlaminar properties. Additionally, composites that have sustained damage often have non-visible or barely-visible damage, complicating damage assessment. Recent efforts to address the limitations of advanced composites include the incorporation of carbon nanotubes (CNTs) to take advantage of intrinsic and scale-dependent properties of these nanostructures. The work reported here builds on a hybrid composite architecture developed in our lab; a fuzzy-fiber laminate[1] that strategically places aligned CNTs throughout the laminate to address mechanical limitations seen with traditional composites. Here, a multifunctional attribute of the nano-engineered hybrid composite is explored to assess the potential of damage sensing using enhanced electrical conductivity of the laminate. Damage increases resistance to electrical conduction, and therefore changes in resistance can potentially be used to sense damage. This sensing system can potentially be integrated into an overall integrated vehicle health management (IVHM)

[1] Graduate Student, Dept. of Aeronautics and Astronautics, 77 Massachusetts Ave. 41-317, Cambridge MA, 02139, and AIAA Student Member.
[2] Postdoctoral Associate, Dept. of Aeronautics and Astronautics, 77 Massachusetts Ave. 41-317, Cambridge MA, 02139.
[3] Associate Professor, Dept. of Aeronautics and Astronautics, 77 Massachusetts Ave. 33-314, Cambridge MA, 02139, and AIAA Member. wardle@mit.edu
[4] President & CEO, Metis Design Corp, 10 Canal Park, Suite 601, Cambridge, MA 02141.
[5] Research Engineer, Metis Design Corp, 10 Canal Park, Suite 601, Cambridge, MA 02141.

approach as *in situ* structural health monitoring (SHM). Such a concept is investigated in this work and the basic principles demonstrated, including both in-plane and through-thickness damage sensing, giving a non-destructive tomographic view of the three-dimensional damage state.

Nano-engineered composites allow control of the location and orientation of CNTs to optimize reinforcement directions. Here, CNTs are arranged radially on the surfaces of advanced fibers and infiltrated with epoxy to create 'fuzzy-fiber' reinforced plastics (FFRP)[1,2], as shown in Figures 1 and 2. While the CNTs occupy <3% of the volume of these bulk nanostructured composites, due to alignment and distribution, significant strength and toughness enhancement has been observed[4,5], in agreement with theoretical models in the case of toughness[6]. A multifunctional aspect of these materials is electrical conductivity that is enhanced by many orders of magnitude ($10^6$ and $10^8$, in-plane and through thickness, respectively)[1,7,8]. This multifunctional aspect is utilized to solve challenges in a resistive structural health monitoring (SHM) sensing concept, *i.e.,* damage causes immeasurable resistance changes in typical polymeric laminated composites because the composites are insulating, whereas laminates containing CNTs have enhanced conductivity such that damage causes measurable changes in resistance as measured over mm to cm lengthscales.

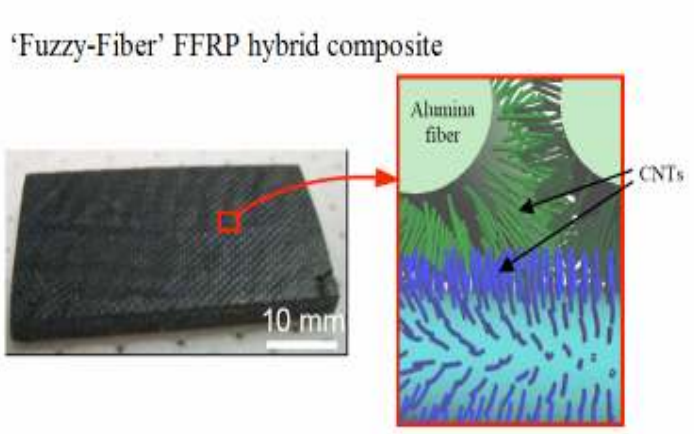


**Figure 1. Laminate composed of cloth containing fibers (in tow form) with *in situ*-grown aligned CNTs in a polymer matrix (left), and illustration of cross-sectional region between tows (right). CNTs grown on the surface of each fiber interact with CNTs of nearby fibers achieving inter-tow and interlaminar reinforcement[3].**

Composites present significant challenges for inspection due to their heterogeneity and anisotropy, the fact they fail by interacting modes, and since damage often occurs beneath the surface (where inspections, particularly visual, take place). Current effective laboratory non-destructive methods, such as X-ray and C-scan, are impractical for inspection of large integrated structures. Resistive SHM methods have been investigated previously, but they are hindered by small measurements (high resistivity giving rise to high noise-to-signal) and interconnection issues. Both issues can be addressed by the increased conductivity in the nano-engineered composites and by creating electrical break-out connections on the surface. Therefore, CNTs serve as multifunctional enhancement: while reinforcing matrix regions between fibers and between plies is the primary objective, secondarily, percolating conductive networks are created that vastly improve conductivity of the bulk composite material. Such enhanced conductivity enables advanced structural health monitoring techniques that may detect internal damage before it can be visually identified as in a typical aircraft inspection.

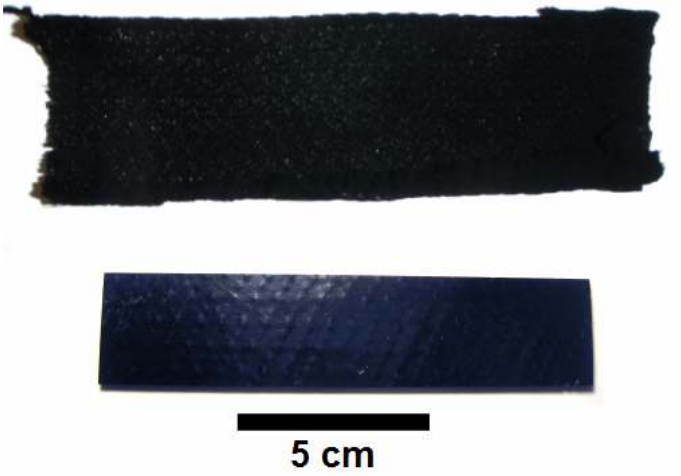


**Figure 2. A fuzzy fiber ply (top) and FFRP laminate (bottom).**

Structural health monitoring (SHM) has been established as a route to assess the level of damage in a composite without relying solely on visual inspection. CNT-enhanced composites show promise to improve the conductivity of composites allowing for monitoring systems that can measure changes in resistance in real time to discover local damage before catastrophic failure[9,10]. Thostenson and Chou built CNT-enhanced advanced fiber-reinforced composites with improvements in electrical conductivity and had encouraging results in damage monitoring using passive in-plane electrical resistance measurements[11]. However, their approach to incorporating CNTs in the fiber-

reinforced composite results in random alignment of short and very low volume fraction CNTs, resulting in little improvement in mechanical properties. Further, their coupon-level approach to SHM used *in-plane* resistance measurements that would require a dense network of invasive wiring and instrumentation for practical large-area monitoring. Thus, a novel approach to incorporating CNTs in fiber-reinforced aerospace structural composites for damage detection, and potentially SHM, is implemented here, whereby all the potential advantages of CNTs are used for improving mechanical properties as well as enabling SHM, with a less invasive electrode network.

The present investigation built on prior work to instrument nano-engineered laminates with a non-invasive silver-ink electrode grid and multiplexing micro-switches connected to compact hardware for through-thickness resistance measurement. The painted electrode grid, inspired by flat panel liquid crystal display (LCD) technology, uses an "active" layer of electrode columns on one surface of the laminate as positive electrode, and on the other surface, another layer of electrode rows will act as "passive" ground (see Figure 3). Thus, by selecting a particular row and column, local through-thickness resistance measurements can be obtained for a grid of points over the structure. Furthermore, in-plane surface resistivity changes at a grid point can be obtained by probing resistance between 2 adjacent traces pairs closest to the point on either surface. As one would intuitively expect, damage in the form of delaminations or cracks will affect the CNT conductive network around the affected zone in the structure, and correspondingly the local through-thickness (and in-plane) resistivity[12,13]. Using the electrode grid and interpolating from the measurements at distinct grid points, high-resolution resistance maps over large structural areas can be obtained, allowing accurate localization of damage.

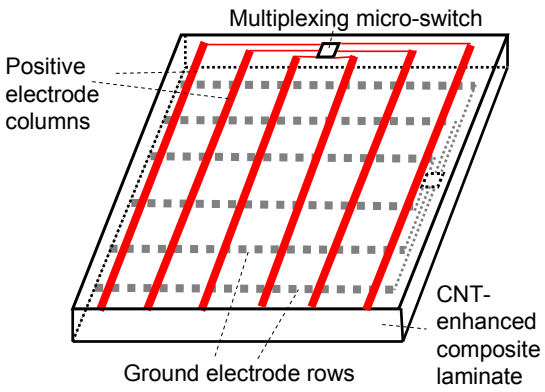


**Figure 3. Schematic of non-invasive silver ink electrode and multiplexing switch network for through-thickness and in-plane resistance measurements of the CNT-enhanced composite laminate.**

## II. Experimental Methods

The first step to manufacture FFRP laminates involves growing CNTs directly on fibers in an alumina fiber woven cloth using a modified thermal chemical vapor deposition (CVD) method developed in previous work[14]. A thick alumina fiber satin-weave cloth is first dipped in a solution of 50mM iron nitrate in isopropanol for 5 minutes and dried in air for at least 8 hours. This catalyst application method allows the catalyst to coat fibers inside the tows of the ply, ultimately distributing CNT growth to all areas of the woven ply (see left side of Figure 2). In a CVD furnace, the catalyst is conditioned to form nanoparticles, or seeds, from which CNTs grow radially aligned and perpendicular to the surface of the fibers. They extend into the matrix to provide reinforcement both within each ply (intralaminar) and between plies (interlaminar). The CNTs grown are typically 20 to 50 μm in length, longer than typical interlaminar spacing (~ 10 μm) and intralaminar spacing (~ 1-5 μm)[15].

FFRP laminates were fabricated using hand lay-up, and the matrix system used was West Systems™ Epoxy, Resin 105 and Hardener 206. In hand lay-up, a ply is laid down on a sheet of non-porous Teflon (GNPT) and epoxy is coated over the surface. The epoxy is wicked into the interior of the woven ply within a few seconds after which another ply is placed on top. In this work, after plies are stacked, porous Teflon (PT), absorbent bleeder paper, and GNPT are placed over the laminate. A caul plate and vacuum are then used to provide pressure to the assembly to ensure uniform thickness. The sample is then left to cure for 12 hours at room temperature. The resulting specimens have ~1% void fraction and a fiber volume fraction of ~50%. The resulting composites are trimmed with a diamond-grit wet cutting wheel[15].

Initially, a single FFRP laminate (114 mm x 25 mm x 3 mm) was tested to demonstrate the overall sensing concept and observe the order of resistance change due to damage from impacting the specimen. Silver-ink electrodes were painted onto the specimen surfaces using simple tape masks. On the top plate surface, 14 parallel conductors were patterned in the short-dimension. On the opposite surface, 4 parallel conductors were patterned in the long dimension, so that they were perpendicular to the top side conductors when projected virtually through the thickness. These traces were all 1.5 mm wide and spaced 3 mm edge-to-edge. Prior to testing, the electrical resistance of each specimen was measured using a Fluke™ 189 model multimeter with resolution 0.01 Ω and accuracy of ±0.05%. Initial data showed significant variability when probing directly on the silver traces.

Subsequently, a procedure was developed to bond thick gauge wires to the traces using silver epoxy, resulting in < 1% change (< 0.1 Ω for ~10 Ω trace) across 10 repeat trials. The specimen with bonded gauge wires was centrally impacted with a 12.7 mm diameter steel ball using a guided dropped weight to initiate damage. The specimen was supported on the backface (away from the impact site) by a wooden block providing a non-specific boundary condition. Following impact, post-damage resistance measurements were collected for each possible trace combination.

Following the initial test, three further FFRP laminates were then tested using a new setup, with several refined processes. First, the silk-screening process was improved to reduce trace resistance and variability, both of which improved measurement accuracy. This was accomplished by selecting a slightly different silver formulation, as well as testing various measurement thicknesses to determine an appropriate value that increases repeatability and was less sensitive to layer tolerances. A chemical etched template was used to apply the proper pattern with better precision. More traces were applied to these specimens for increased spatial resolution (32 horizontal and 8 vertical as opposed to 14 x 4) by greater than a factor of 4. All traces were still 1.5 mm wide, but this time the traces were spaced by 1.5 mm rather than 3 mm. Rather than using soldered wires to connect to the traces, a single double-sided copper-coated Kapton flexible circuit with overlay was designed to make connections with the direct-write traces. In a process developed recently in a NASA Phase I SBIR by Metis Design Corp., the flex circuit was bonded to the specimens first, then the direct-write traces were applied to the specimens, including overwriting the flex-circuits (which included alignment marks)[16]. A urethane coating was applied to prevent oxidation. The flex circuit was designed in the shape of a rectangular frame, with flaps on all 4 inside edges with exposed pads for the direct-write process. The specimens fit inside the frame window with the top and bottom flap overlapping onto the front of the FFRP, and the left and right flap overlapping on the back of the FFRP. Traces are then routed along the edges of the frame to an 80 pin ZIF connector located on a bottom tab for hardware connection. This "flex-frame", as seen in Figure 4, provides electrical continuity from traces to hardware with more reliability, durability and consistency than the prior method, specifically because it eliminates all measurable contract resistance issues. Finally, a PC board was designed to mate with this flex-frame, containing switches to multiplex the channels and reliable connections for a multimeter probe and PC readout. After being instrumented, each FFRP specimen was progressively impacted at 15, 30 and 45 ft-lbs, using the same guided drop-weight setup, with in-and-out-of-plane resistance measured after each subsequent impact. The guided impactor did not ensure central impact and variability in the location of "central impact" was observed both visually and in the sensed damage as will be discussed below. The impactor was also uninstrumented, so the peak force and impact histories are not available.

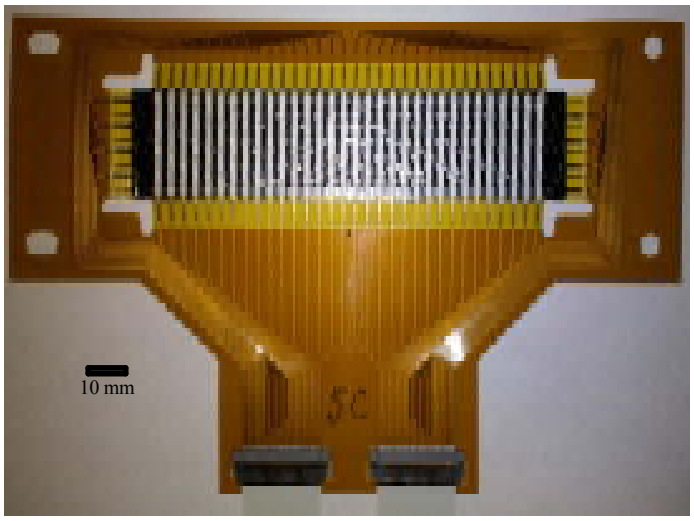


**Figure 4. FFRP specimen mounted in "flex frame" used to break out direct-write electrodes to data collection ports (ZIF connector).**

## III. Results and Discussion

Results from both preliminary testing as well as final testing of three FFRP specimens using the improved direct-write trace and flex-frame hardware are presented here. In initial testing with the hand-painted silver-ink electrodes, no damage was visible to the unaided eye after impact, however, optical microscopy revealed cracking on the front surface of the laminate. Two sets of resistance data were collected: 1) in-plane between each parallel pair of adjacent traces, and 2) through-thickness at each grid point created by the virtual intersection of the perpendicular top and bottom surface traces. For the in-plane resistance, the short trace average resistance was 9 Ω pre-impact. Note that both in this initial testing and in subsequent testing, baseline specimens without CNTs registered an open circuit (very high resistance that was immeasurable given the acquisition equipment). Following impact, while the outermost trace pairs on either side of the damage site along the x-axis showed < 10% change, the middle was

consistently > 100%, as seen in Figure 5(a). Minor changes < 1% were detected between long trace pairs. For the 56 through-thickness grid points, pre-impact resistance values averaged 20 Ω. As seen in Figure 5(b), a clear change of > 100% was detected in the impacted region. Along the x-axis, between the measurement points for the long traces (left edge in Figure 5(b)) and the damage site, < 10% change was observed. However on the opposite side of the damage site (right side of Figure 5(b)), a constant resistance offset was introduced due to the presence of cracks across the electrodes. An important aspect of future work will be to develop approaches that differentiate between trace damage and laminate damage. The initial testing demonstrated that the FFRP laminates, with enhanced conductivity, can be used in such a 3D damage sensing scheme and tomographic-like damage state images were generated associated with post-impact damage.

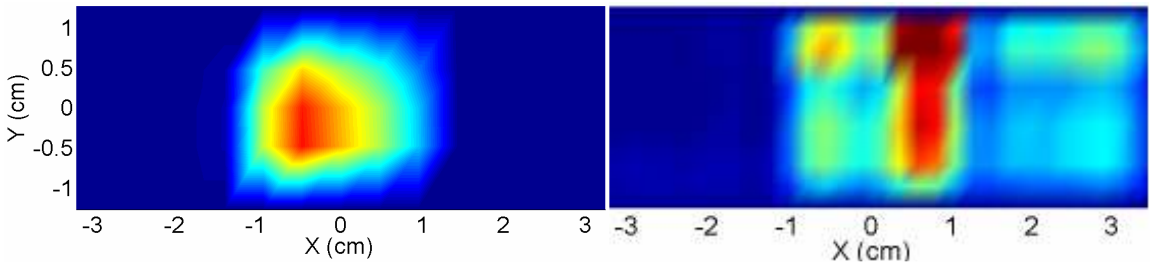


**Figure 5: Initial test results for centrally impacted FFRP specimen: (left) in-plane resistance % change image generated by multiplying and interpolating top/bottom adjacent parallel trace measurements, and (right) through-thickness resistance % change image generated by interpolating grid point measurements.**

Subsequent to the completion of the initial testing, three further tests were completed with the improved trace and data acquisition hardware. The focus of this series of experiments was to use the improved data acquisition to confirm the initial damage sensing results and to investigate progressive near-central impact damage. Again, central-impact was not assured given the impact setup and furthermore only impactor energy is available to scale the results. Following the procedure previously described, each of the three specimens were impacted at 15, 30 and 45 ft-lbs, with resistance data collected between each trial. Overall, the results from the refined setup validated the initial test results, demonstrating that the CNT's provide an excellent indication of barely visible impact damage (BVID). Furthermore, as can be seen in Figure 6, the overwhelming outcome was that with each progressive impact level, additional disruption (due to damage) of the CNT electrical network resulted in a nearly linear increase in peak % change of resistance value. For in-plane resistance, the first impact caused barely perceivable, but repeatable changes of ~10-20% in the impact region. The second impact caused ~20-30% resistance change, and the final impact ~40-60% change. In-plane results appeared to be more localized to the actual impacted region, with clearly distinguishable damage patterns radiating from the impact center. Once locked into place, the impact location for progressive impacts on the same specimen was always in the same location, however due to some play in the guiding system for the dropped weight, the impact location specimen-to-specimen was not always in the same location. This effect may be seen by comparing specimen 2 which had the best central alignment, with specimen 3, which was impacted towards the bottom edge. The specimen-to-specimen variability in measured damage was also likely influenced by the actual impact point, as a central impact would typically gives a more uniformly distributed state of damage in the specimen and cause less edge crushing. Clearly, controlled impact with data acquisition is a key area for improvement in the testing procedures.

For through-thickness results, the initial impact again caused small changes of ~2-4%, with the second impact causing ~4-8% changes and the final impact registering ~8-10% changes. In this case, the pattern of the results appeared to be much less sensitive to impact location, likely because these were relatively narrow specimens. However, the damage severity measured did seem dependant on the impact point. The improved setup appeared to resolve the issue observed in the initial test results for the through-thickness measurements, where no DC off-set was calculated to the "right" of the damage region due to electrode cracking. No visible damage was present in any of these cases. Last, it should be noted that the resistance-based damage sensing was not coupled with other NDE/I methods to make comparative assessments of the resistance measurements to traditional methods of visualizing damage due to time constraints. Further work should focus on more consistent and repeatable specimen manufacturing, likely utilizing newly developed and improved fabrication via resin infusion[17] as recently demonstrated. Furthermore, traditional damage inspection techniques such as x-radiography, C-scan, sectioning, and

computed tomography should be coupled with the resistance-based method to ascertain spatial and modal correlation of the sensed damaged via electrical resistance.

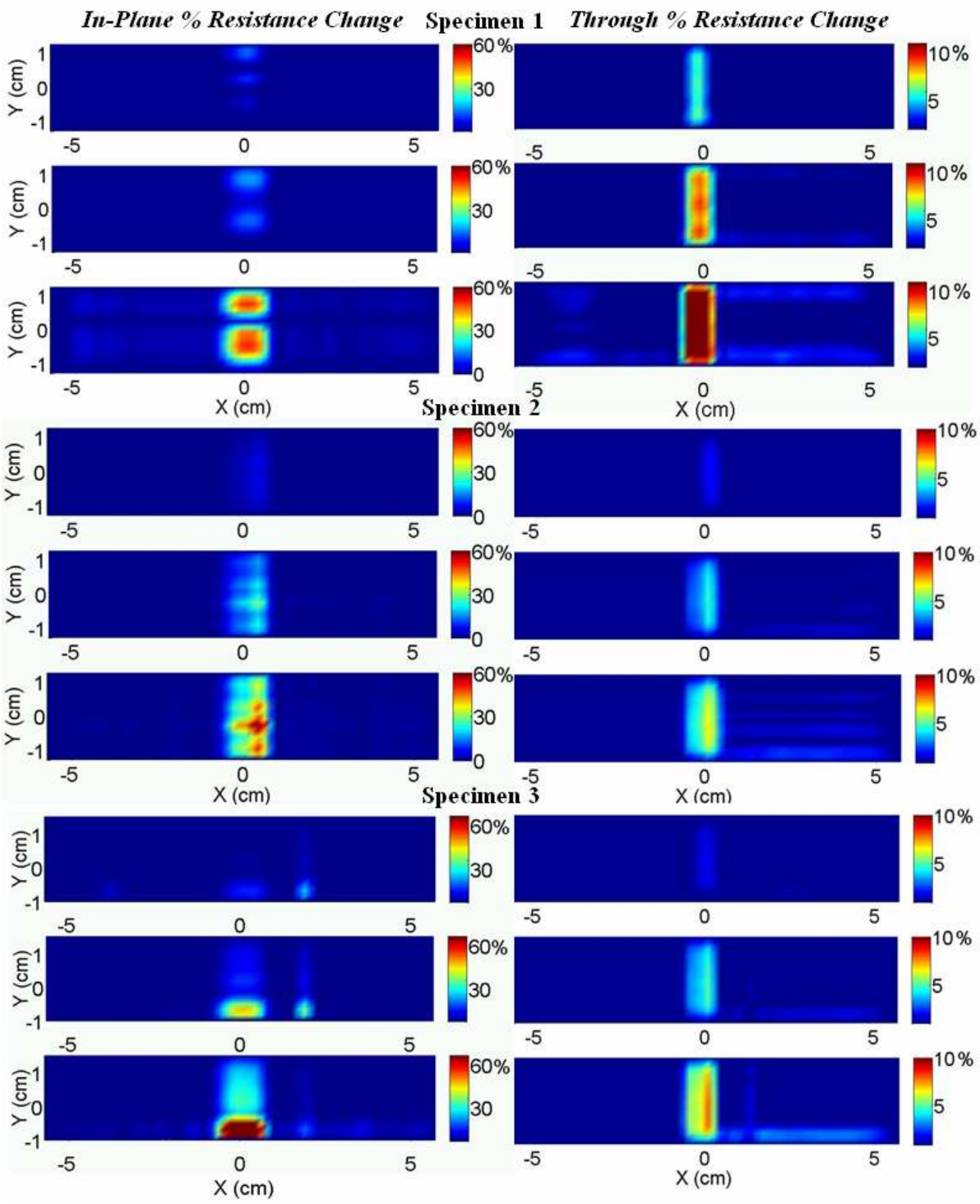


**Figure 6. Impact-induced % change in resistance values. Left column displays in-plane results and right column displays through-thickness results. First plot in each set presents changes following 15 ft-lbs impact, second follows 30 ft-lbs and third presents results following 45 ft-lbs impact.**

## IV. Conclusions and Recommendations

CNT-enhanced composites were fabricated, patterned with a silver ink electrode grid, and subsequently subjected to impact damage. Both in-plane and through-thickness electrical resistance measurements were collected. Clear changes were observed in both sets of data for grid lines close to the impacted zone of the specimen, demonstrating that these parameters were sensitive to damage in the structure. The peak resistance changes were close to the center of the specimen near the impact site, and little to no change was observed in values at points away from the damage zone. Overall, the sub-surface impact damage caused significant electrical resistance changes, allowing for a full-field representation of the damage locations by interpolating the collected data. The results indicate that the different resistance changes are sensitive to different damage modes, but further work is needed to substantiate this initial observation. As an example, in-plane resistivity may be more sensitive to surface cracks, which tend to form at the edge of the impact zone. Conversely, through-thickness resistivity may be more sensitive to delamination, which would affect the CNT conductive network across the specimen plies. This work demonstrates the potential of using this approach as an SHM solution, with the added benefit of CNTs reinforcing the structure (see summary of mechanical, electrical, and thermal improvements for the alumina-fiber FFRP system in Ref. 17). These initial results provide an excellent foundation for research to further scale and mature this damage detection technology. Several recommendations for future work have been suggested throughout the body of the manuscript, including impact tests that are more rigorously controlled, and comparison of the electrical-resistance tomographic damage maps to traditional composite damage inspection techniques such as x-radiography and C-scan. Additional work on relevant composite systems such as carbon fiber FFRP systems is also recommended[18].

## Acknowledgments

This research was sponsored by the Air Force Office of Scientific Research, under the Phase I STTR contract FA9550-09-C-0024. The work was performed at the Metis Design Corporation in Cambridge, MA, with a subcontract to the Department of Aeronautics and Astronautics at MIT, in Cambridge, MA. The nano-engineered composites used in this work were developed by MIT's Nano-Engineered Composite aerospace STructures (NECST) Consortium with support from Airbus S.A.S., Boeing, Embraer, Lockheed Martin, Saab AB, Spirit AeroSystems, Textron Inc., Composite Systems Technology, and TohoTenax.

## References

[1]Garcia, E. J., Wardle, B. L., Hart, A. J., and Yamamoto, N., "Fabrication and Multifunctional Properties of a Hybrid Laminate with Aligned Carbon Nanotubes Grown In Situ," *Composites Science and Technology,* Vol. 68, No. 9, 2008, pp. 2034-2041.

[2]Garcia, E. J., Hart, A. J., Wardle, B. L., and Slocum, A., "Fabrication and Testing of Long Carbon Nanotubes Grown on the Surface of Fibers for Hybrid Composites," *47th AIAA/ASME/ASCE/AJS/ASC Structures, Structural Dynamics, and Materials Conference Proceedings*, Newport, R.I., May 1-4, 2006.

[3]Wardle B. L., et al., "Particle and Fiber Exposures During Processing of Hybrid Carbon-Nanotube Advanced Composites," *2008 SAMPE Fall Technical Conference Proceedings*, Memphis, TN

[4]Garcia, E. J., Hart, A. J., and Wardle, B. L., "Long Carbon Nanotubes Grown on the Surface of Fibers for Hybrid Composites," *AIAA Journal*, Vol. 46, No. 6, 2008, pp. 1405-1412.

[5]Wicks, S. S., Guzman de Villoria, R., and Wardle B. L., "Interlaminar and Intralaminar Reinforcement of Composite Laminates with Aligned Carbon Nanotubes," *Composites Science and Technology,* Vol. 70, No. 1, 2010, pp. 20-28.

[6]Blanco, J., Garcia E. J., Guzman deVilloria R., and Wardle, B.L., "Limiting Mechanisms in Mode I Interlaminar Toughness of Composites Reinforced with Aligned Carbon Nanotubes," *J. Composite Materials,* Vol. 43, No. 8, 2009.

[7]Yamamoto, N., Garcia, E. J., Wardle, B. L., and Hart, A. J, "Thermal and Electrical Properties of Hybrid Woven Composites Reinforced with Aligned Carbon Nanotubes," *49th AIAA Structures, Dynamics, and Materials Conference Proceedings*, Schaumburg, IL, April, 7-10, 2008.

[8]Yamamoto, N., Guzmán de Villoria, R., Cebeci, H., and Wardle, B. L., "Thermal and Electrical Transport in Hybrid Woven Composites Reinforced with Aligned Carbon Nanotubes," *51st AIAA Structures, Structural Dynamics, and Materials (SDM) Conference Proceedings*, Orlando, FL, April 12-15, 2010.

[9]Thostenson, E.T. and Chou, T.-W., "Real-time in situ sensing of damage evolution in advanced fiber composites using carbon nanotube networks," *Nanotechnology,* Vol. 19, No. 21, 2008, p. 215713.

[10]Li, C., Thostenson, E. T., and Chou, T.-W., "Sensors and actuators based on carbon nanotubes and their composites: A review," *Composites Science and Technology,* Vol. 68, No. 6, 2008, pp. 1227-1249.

[11]Thostenson, E. T., Chou, T.-W., "Carbon Nanotube Networks: Sensing of Distributed Strain and Damage for Life Prediction and Self Healing," *Advanced Materials,* Vol. 18, No. 21, 2006, pp. 2837-2841.
[12]Raghavan, A., et al. "Structural Health Monitoring using Carbon Nanotube (CNT) Enhanced Composites". *7th International Workshop on Structural Health Monitoring Proceedings*, Stanford University, Sept. 9-11 2009.
[13]Barber, D. M., et al. "Health Monitoring of Aligned Carbon Nanotube (CNT) Enhanced Composites," *2009 SAMPE Fall Technical Conference Proceedings*, Wichita, KS, Oct. 2009.
[14]Yamamoto, N., et al., "High-yield growth and morphology control of aligned carbon nanotubes on ceramic fibers for multifunctional enhancement of structural composites" *Carbon,* 2008.
[15]Wicks, S. S., Guzman de Villoria, R., Barber, D. M., and Wardle, B. L., "Interlaminar Fracture Toughness of a Woven Advanced Composite Reinforced with Aligned Carbon Nanotubes," *50th AIAA/ASME/ASCE/AHS/ASC Structures, Structural Dynamics, and Materials Conference Proceedings*, Palm Springs, CA, May 4-7, 2009.
[16]Kessler, S. S., Raghavan, A., Dunn, C. T., and Wardle, B.L., "Health Monitoring of Carbon Nanotube (CNT) Enhanced Composites", *USAF Report FOSR-NA-2010-1790*, March 2010.
[17]Wicks SS, Ishiguro K, Guzmán de Villoria R, and Wardle BL. Mechanical Properties of Infusion-Processed Fiber Reinforced Plastics with *In Situ* Grown Aligned Carbon Nanotubes. *51st AIAA Structures, Structural Dynamics, and Materials (SDM) Conference Proceedings*, Orlando, FL, April 12-15, 2010.
[18]Steiner III, S.A., et al. "Methods for Growing Carbon Nanotubes on Carbon Fibers that Preserve Fiber Tensile Strength," *51st AIAA Structures, Structural Dynamics, and Materials (SDM) Conference Proceedings*, Orlando, FL, April 12-15, 2010.